Acoustic emission analysis coupled with thermogravimetric experiments dedicated to high temperature corrosion studies on metallic alloys

Véronique Peres, Omar Al Haj, Eric Serris, Michel Cournil, François Grosjean, Jean Kittel, Francois Ropital

Acoustic emission analysis coupled with thermogravimetric experiments dedicated to high temperature corrosion studies on metallic alloys

PERES Véronique, AL HAJ Omar, SERRIS Eric, COURNIL Michel, Ecole Nationale Supérieure des Mines, SPIN-EMSE, PRESSIC-Department, CNRS:UMR 5307, LGF, 42023 Saint-Etienne France,

GROSJEAN François, KITTEL Jean, ROPITAL François, IFP Energies nouvelles, Rond-point de l'échangeur de Solaize BP3, 69360 Solaize France.

Summary

High temperature corrosion of metallic alloys (like Iron, nickel, cobalt alloys) can damage equipment of many industrial domains (refinery, petrochemical …). It represents a major challenge. Acoustic emission (AE) is an interesting method owing to its sensitivity and its non-destructive aspect to quantify the level of damage in service of these alloys under various environmental conditions. High temperature corrosive phenomena create stresses in the materials; the relaxation by cracks of these stresses produces transient elastic waves which can be recorded and analyzed using the AE system. The study of these transient waves enables the anticipation of the degree of damage of the alloys. Several methods are used to record and analyze these transient elastic waves. Piezoelectric sensors fixed directly on the structure can be used. But in case of high temperature environments, a waveguide may be used to transmit waves from the sample to the sensors. Our study establishes an acoustic signals database which assigns the acoustic signals to the specific corrosion phenomena. This database will be useful for the monitoring of industrial equipment using acoustic emission methods. For this purpose, thermogravimetric analysis (TGA) has been coupled with acoustic emission (AE) devices. Simultaneous measurements of the mass variation and of the acoustic signals emitted during the corrosion of samples at high temperature provide complementary information. For this purpose a specific alumina waveguide (WG) has been developed.

The oxidation of a zirconium alloy, zircaloy-4, was firstly studied using thermogravimetric experiment coupled to acoustic emission analysis to validate the waveguide operation at 900 °C. Metal dusting represents also a severe form of corrosive degradation of metal alloy. Iron metal dusting corrosion, with or without pre-oxidized layer, was studied by EA coupled with TGA at 650°C under C_4H_{10} + H_2 + He atmosphere.

From these studies we can conclude that reversible mechanisms are not emissive. Irreversible mechanisms, as cracks initiation and propagation, are audible.

1 Introduction

Over the last few decades several authors have been studying high temperature corrosion behaviour of metals and alloys, steels sulfidation [1], metal dusting inhibition [2], and alloys oxidation [3] using the acoustic emission devices. Since

1977 other authors have coupled acoustic emission with thermogravimetric analysis (TGA) in order to improve the knowledge of different high temperature corrosion phenomena [4-8]. The sample mass variation and the AE signals are simultaneously recorded over these experiments.
In this study, we use an innovative device to perform such experiments with based on TGA analysis coupled with in situ acoustic emission. We record samples mass variation and the AE signals during the oxidation at high temperature of a zirconium alloy, Zircaloy-4 and also during metal dusting of pure iron.

2 Experimental

Thermogravimetric analyses were carried out on a symmetric thermobalance (SETARAM TAG 24) with Pt-Rh 6%/ Pt-Rh 30% thermocouples, in order to measure the specimen's mass change during the corrosion tests with a precision of ± 0.001 mg.

The experiments were performed on a zirconium alloy , Zircaloy-4 platelet specimens (4.8 mm x 4.6 mm x 0.5 mm) and iron platelet (4.4 mm x 4.6 mm x 1 mm). The chemical compositions of those materials are given in Table 1 and 2. Samples were polished and cleaned with acetone and ethanol before the oxidation tests.

Table 1 : Chemical composition of Zircaloy-4 (weight%)

Sn	Fe	O	Cr	C (ppm)	Zr
1.32-1.35	0.21	0.123-0.129	0.11	125-140	Bal

Table 2 : Chemical composition of alloy elements (ppm) in pure iron

C	Cr	Si	Al	Ti	Mo
2	0.94	0.18	0.19	0.05	0.03

Zircaloy-4 oxidation tests were done at 900°C ± 0.1°C (this temperature is in the field of accidental conditions in the nuclear power plants); the heating rate was 15°C/min in pure helium. The isothermal dwell time was fixed to 5 hours. Once the dwell temperature was reached, helium was switched to a mixture of (75% He + 21% O_2 + 4% N_2) for the first series of oxidation tests, another oxidant gas was used (80% He + 20% O_2) for the second series of oxidation tests. In both series the oxidant gas was introduced by mass flow meters with a total gas flow rate of 50 ml/min. The cooling rate was 15°C/min under the same process gas mixture.
For pure iron metal dusting tests the temperature was fixed at 650°C ± 0.1°C; the heating rate was 15°C/min in pure helium. The isothermal dwell time was fixed to 24 hours. Once the maximum temperature was reached, helium was switched to a mixture of (90% He + 5 % iC_4H_{10} + 5 % H_2 : carbon activity ac>1). The cooling rate was 15°C/min under helium.
A specific acoustic device (waveguide) has been developed to optimize the transmission of the acoustic signals from samples (AE source) to the sensors (Figure

1). The waveguide was conceived according to the following criteria: i) chemical resistance against corrosive environments (oxygen or carbon-reductive atmospheres); ii) chemical inertness with regard to the alloy samples; iii) good transmission of the acoustic signals via the waveguide (low attenuation of the signal energy); iv) optimization of the contact between the sample and the waveguide. The waveguide dimensions are compatible with the internal diameter of the furnace and with the maximal weight that can be supported by the thermobalance. Specimens had been placed directly on the waveguide; another waveguide without specimens had been placed in the reference furnace of the thermobalance in order to minimize the baseline shift during experiments and to keep the symmetric aspect between the two parts of the thermobalance.

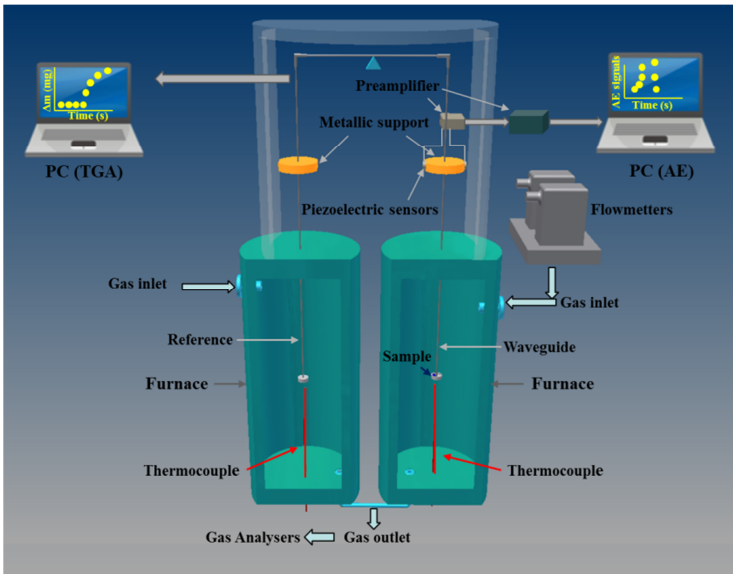

Fig. 1. Symmetric thermobalance (TGA 24) coupled with acoustic emission devices

AE piezoelectric sensors were linked to the waveguide via a metallic support; sensors and metallic support were placed inside the cold part of the thermobalance where the temperature does not exceed 150°C. The sensors are linked to an acquisition chain controlled by the AEwin™ software and data were analysed using Noesis™ software provided by the Physical Acoustics Corporation Company. The characteristics of the acquisition chain are given in Table 3. The threshold is very low fixed to 18 dB_{AE}.

Table 3 : Main characteristics of the AE acquisition chain

Instrumentation	Sensors	Threshold (dB_{AE})	System filter (KHz)	Model of the amplifier	Sampling rate	PDT - HDT - HLT
Characteristics	PICO 30	18	10 - 1200	2/4/6 gain : 60 dB_{AE}	0.25 µs (4MHz)	100 - 200 - 400 (µs)

Discontinuous acoustic emission analysis (AE burst) has been used during this study. At ambient temperature, the normalized Hsu-Nielsen test was carried out to verify the AE system.

Blank tests at 900°C without any specimen were carried out to validate that the waveguide did not significantly react with the gas mixture. During these tests, the stability of the mass signal confirms the chemical inertness of the waveguide. Blank

tests allow us to distinguish the acoustic emission signals which result from the instrumental noise (IN). They are characterized by a very short duration and a low number of counts, 95% of these bursts are characterized by 1 count and a duration of 1 µs. They are also characterized by a high average frequency in the range of 200 kHz to 1000 kHz including the resonance frequency of the sensors (300 kHz). Burst's absolute energy is very low and doesn't exceed 0.1 aJ/burst. These instrumental noise AE bursts have been deleted from the acoustic emission analysis for the rest of the study.

3 Result

3.1 Zircaloy-4 corrosion

3.1.1 Oxidation tests under air

Figure 2 shows the bursts amplitude recorded during the Zircaloy-4 oxidation tests under air (75% He + 21% O_2 + 4% N_2) and the kinetic rate variation as function of time. According to the kinetic rate curves, we note that AE bursts have been recorded just after the kinetic transition (breakaway [9-10]) occurring 40 minutes after the introduction of the oxidant gas mixture. Each time an important AE activity, called post-transition bursts, appears just after the breakaway. Post-transition bursts recorded during the temperature dwell time are characterized by mean amplitude in the range of 18 to 40 dB_{AE}. AE bursts possess a low average frequency varying between 1 kHz to 200 kHz. Their absolute energy average is about 10 aJ/burst. AE signals were also recorded during the cooling of the sample. AE bursts recorded during this step are more energetic (100 aJ/burst) and characterized by long duration, and high counts number/burst (300 counts/burst).

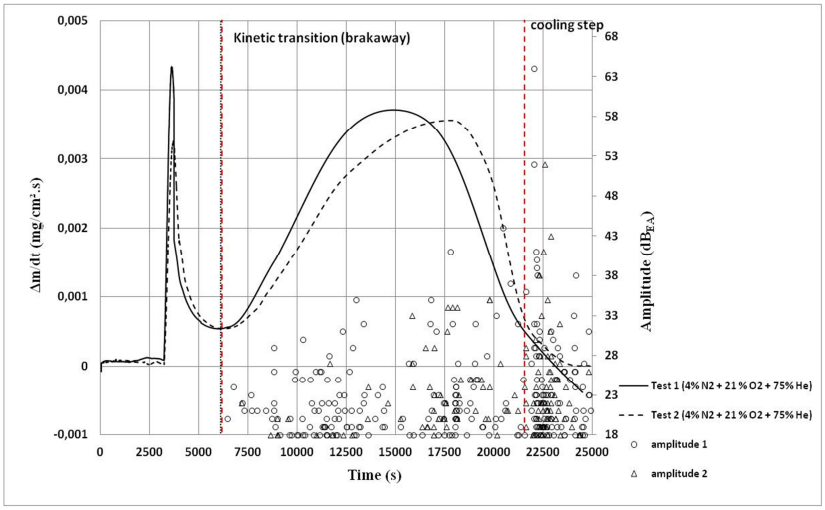

Fig. 2. Rate of mass gain and burst amplitude as a function of time during Zircaloy-4 oxidation tests under 75% He + 21% O2 + 4% N2

SEM cross section of oxidized sample (Figure 3) obtained with scanning electron microscopy (JEOL 6500 F) indicates that cracks are located inside the inward zirconia layer. Type 1 cracks are visible in the external dense

zirconia layer (1). Well distributed thin and convoluted type 2 cracks are observed parallel to the metal oxide interface (2). Type 3 big open cracks are periodically observed perpendicular to the interface totally crossing the zirconia layer (3). The core of the sample remains partially oxidized forming α-ZrO solid solution of oxygen in zirconium according to the zirconium- oxygen binary diagram [11].

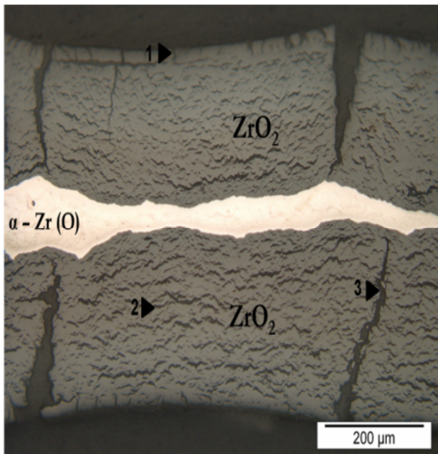

Fig. 3. SEM cross section of Zircaloy-4 oxidized under air at 900°C

Theses cracks can be associated with the AE signals recorded after the kinetic transition. We can attribute the AE bursts to these post-transition stage cracks. Even the AE threshold is low (18 dB_{AE}), the type 2 convoluted cracks parallel to the metal/oxide interface probably do not generate AE signals. The number of type 2 cracks surpasses the amount of AE bursts which have been recorded during the oxidation test. These cracks seem not to be emissive events.

3.1.2. Oxidation tests under oxygen

The kinetic transition doesn't appear during the oxygen test at 900°C (80% He + 20% O_2), the kinetic rate decreases or remains constant throughout the experiment (Figure 4). In order to confirm the absence of the kinetic transition, the dwell time was extended from 5 hours to 10 hours (Figure 3). Results obtained during the extended test confirm the absence of breakaway. The kinetic oxidation under oxygen is defined by a sub-parabolic law. The oxidation process is governed by the oxygen vacancy diffusion through a dense zirconia layer.

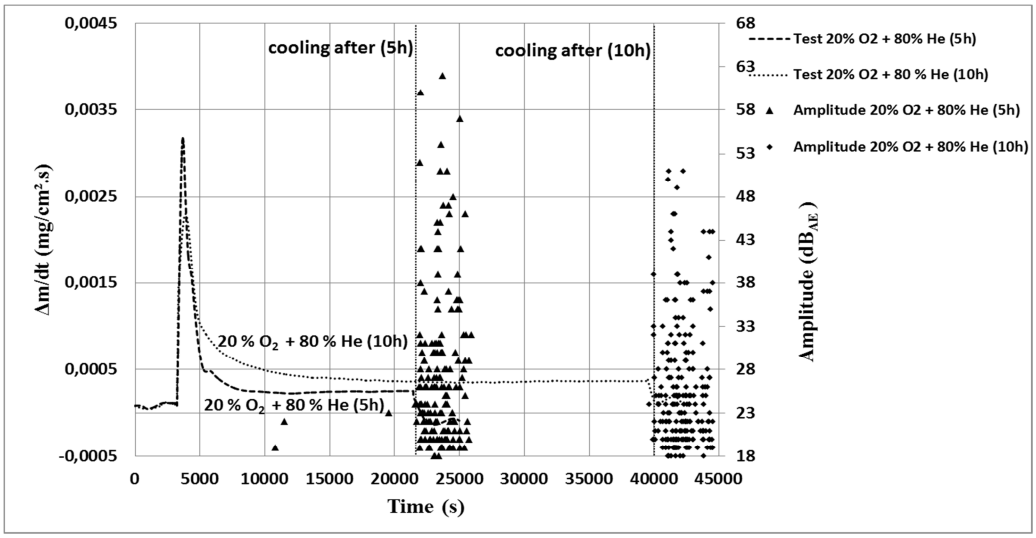

Fig.4. Rate of mass gain as a function of time and bursts amplitude variation during Zircaloy-4 oxidation tests under oxygen (▲) [5 hours] - (♦) [10 hours]

No AE signals were observed during the dwell times. AE bursts recorded appear only during the cooling step. The bursts parameters of these tests are similar (amplitude, counts number, duration, average frequency …). The AE bursts recorded during the cooling step are characterized by a high absolute energy (200 aJ/burst). Their counts' number is in the order of magnitude of hundreds of counts per burst, and their amplitude varying between 20 dB_{AE} and 60 dB_{AE}.

SEM cross section of 5 hours oxidized samples (Figure 5) shows a very dense external zirconia layer. Cracks (1) are only located in the α-Zr(O) scale, which is in white contrast in the metal phase close to the metal/oxide interface. The core of the sample is α-Zr which results from the transformation phase (β-Zr ➔ α-Zr) occurring during cooling.

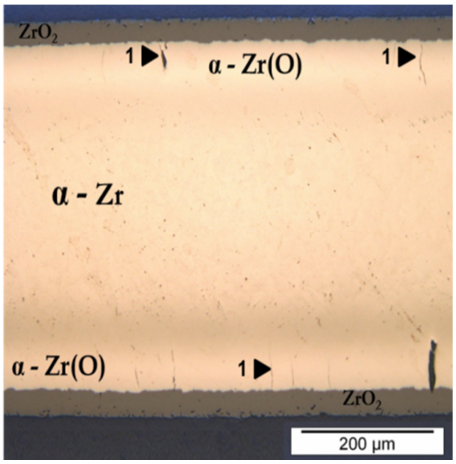

Fig. 5. SEM cross section of Zircaloy-4 oxidized 5 hours under oxygen at 900°C (cracks indicated by "1" indicators)

Considering the micrographs of figure 5, the AE bursts observed during the last part of the cooling may be generated by the cracks observed in the α-Zr(O) layer. Difference in thermal expansion coefficients of α-Zr, α-Zr(O) layer and dense ZrO_2

scale, which are able to create compressive stresses, may explain the cracks which appear during the cooling at temperature close to 400°C.

3.2. Metal dusting

The sample mass gain of metal dusting tests on pure iron is shown as function of time in figure 6. The amplitude of acoustic bursts is also plotted. In the first part of the experiment (up to 40000 s) the sample mass gain is slowly growing up to 1 mg. Then the curve become linear, the total mass gain is nearly 8 mg. 95% of the mass gain is carbon powder deposit at the sample surface. At the beginning of this linear part, the acoustic emission occurs until the end of the test.

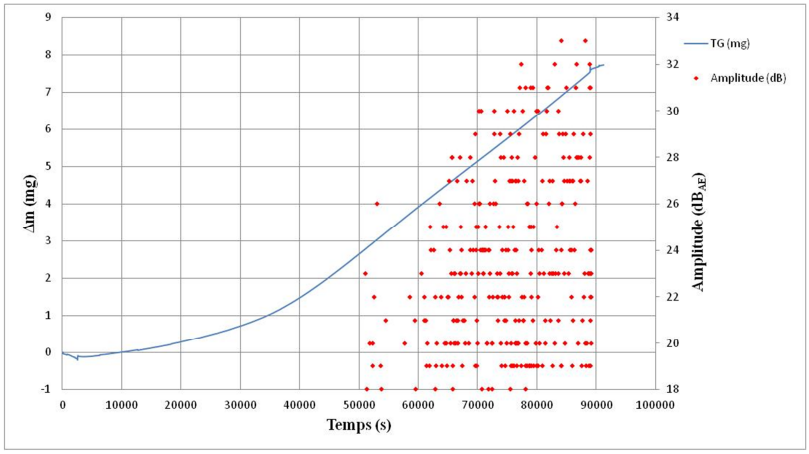

Fig. 6. Typical AE burst waveform continuous wavelets recorded during the cooling of oxidation tests

The metal dusting process can be described with several steps [12]. The first one is carbon dissolution inside the iron matrix. When the activity of carbon inside the iron reaches the activity of formation of cementite (Fe_3C), this phase can form according to this chemical reaction: 3 Fe + C ➔ Fe_3C. When the surface is covered by cementite, a large amount of graphite and coke can deposit on the sample surface. The metastable cementite disintegrates giving iron free particles and carbon pits inside the iron matrix. We can consider that the first step of carbon dissolution is the slow part of mass gain. The carbon deposit with cementite formation and disintegration occur during the linear part of the curve. The acoustic emission begin when the acceleration of sample mass gain correspond to a linear part of the curve (after 50000 s of experiment). The most probable step that may lead to a significant energetic release with acoustic emission bursts is the decomposition of cementite and more precisely the incorporation of carbon inside the iron matrix.

SEM cross section of the iron samples after 24 hours of metal dusting (Figure 7) shows the small carbons pits at iron surface.

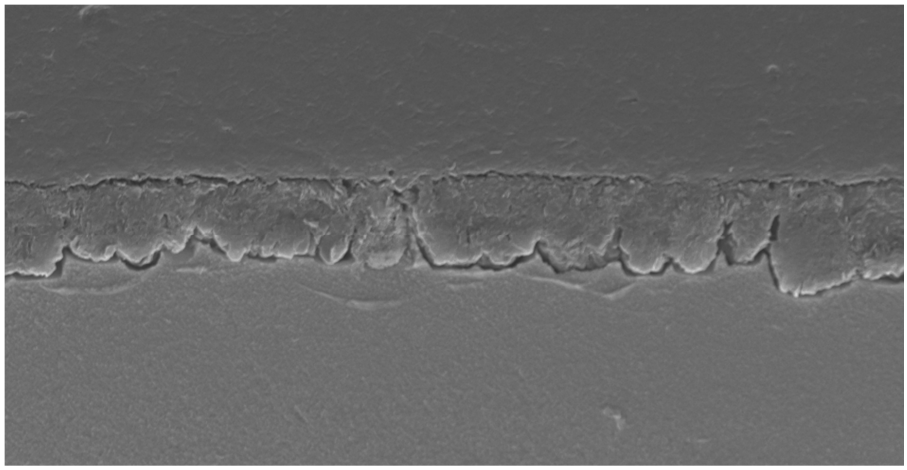

Fig. 7. SEM cross section of pure iron after 24 hours of metal dusting at 900°C

4 Conclusions

Thermogravimetric experiments coupled with acoustic emission analysis are an interesting way to improve knowledge on the corrosion of metallic materials at high temperature.
AE technique allows us to study deeper in details the oxidation behaviour of zircaloy-4 at high temperature. The kinetic transition is detected under air tests at 900°C by a change in the rate of mass gain during the isothermal dwell time. This breakaway is also immediately detected by the AE activity. AE analysis is complementary of post-mortem oxidized samples characterizations. It allows us to distinguish the cracks which occur during the oxidation from the cracks which arise during the cooling of the samples.
We also successfully used this innovative device for petro-chemical applications where metal dusting represents a severe form of corrosion. Metal dusting of iron samples was studied by AE coupled with TGA at 650°C under isobutane and hydrogen. Acoustic emission signals were detected after a significant increase of the sample mass corresponding to carbon penetration in iron.
From these studies we can conclude that mechanisms as diffusion of atoms (oxygen vacancies in case of zirconium inward oxidation in pure oxygen at 900°C) are not emissive. Irreversible mechanisms, as cracks initiation and propagation, generate AE signals.

5 Acknowledgment

This work is a part of the FUI program: IREINE (Innovation for REliability of INdustrial Equipments) dedicated to the development of devices and monitoring services to follow the corrosion of industrial process equipment. This program is founded by the French Rhone Alpes Region.

6 References

[1] M. Shuthe, A. Rahmel and M. Shütze, Oxidation of metals (1998) 33-70.
[2] F. Ferrer, J. Goudiakas, E. Andres and C. Brun, Nace Corrosion Conference, paper 01386 (2001)
[3] M.T. Tran, M. Boinet, A. Galerie, Y. Wouters, Corrosion Science, 52 (2010)2365–2371
[4] R.F. Hochman Proc. of the symp. On Properties of High Temperatures Alloys with Emphasis on Environnemental Effects (Eds. Z.A. Foroulis and F.S. Pettit). The Electrochemical Society (1977) 715
[5] M.J. Bennett, D.J. Buttle, P.D. Colledge, J.B. Price, C.B. Scruby and k.A. Stacey, Materials Science and Engineering, A120 199 (1989)
[6] H. J. Schmutzler and H.J. Grabke, Oxidation of metals, 39 (1992) 15- 29
[7] HJ. Grabke Materials and Corrosion; 1998 (49) 303
[8] F. Grosjean, J. Kittel, F. Ropital, E. Serris, V. Peres, Spectra Analyse 279 (2011), 35-44
[9] M. Tupin, M. Pijolat, F. Valdivieso, M. Soustelle Journal of Nuclear Materials; 342 (2005) 108-118
[10] M. Steinbrück, Journal of Nuclear Materials; 2014 (447) 46-55
[11] J.P. Abriata, J. Garcés, R. Versaci «The O-Zr (Oxygen-Zirconium) system », Bulletin of Alloy Phase Diagrams, 7-2, (1986),116-121
[12] D. J. Young, J. Zhang, C. Geers and M. Schutze, Materials and Corrosion, 62 (2011), 7-28